



N15

12/11/01
11-02
C. J. Steffen
J. R. DeBonis

AIAA-2000-0889

**Numerical Analysis of the Trailblazer Inlet
Flowfield for Hypersonic Mach Numbers**

C.J. Steffen, Jr., and J.R. DeBonis

NASA Glenn Research Center

Cleveland, OH

**38th Aerospace Sciences
Meeting & Exhibit**
January 10-13, 2000 / Reno, NV



Numerical Analysis of the Trailblazer Inlet Flowfield for Hypersonic Mach Numbers

C.J. Steffen, Jr. and J.R. DeBonis
Glenn Research Center, Cleveland, Ohio

The NASA STI Program Office . . . in Profile

Since its founding, NASA has been dedicated to the advancement of aeronautics and space science. The NASA Scientific and Technical Information (STI) Program Office plays a key part in helping NASA maintain this important role.

The NASA STI Program Office is operated by Langley Research Center, the Lead Center for NASA's scientific and technical information. The NASA STI Program Office provides access to the NASA STI Database, the largest collection of aeronautical and space science STI in the world. The Program Office is also NASA's institutional mechanism for disseminating the results of its research and development activities. These results are published by NASA in the NASA STI Report Series, which includes the following report types:

- **TECHNICAL PUBLICATION.** Reports of completed research or a major significant phase of research that present the results of NASA programs and include extensive data or theoretical analysis. Includes compilations of significant scientific and technical data and information deemed to be of continuing reference value. NASA's counterpart of peer-reviewed formal professional papers but has less stringent limitations on manuscript length and extent of graphic presentations.
- **TECHNICAL MEMORANDUM.** Scientific and technical findings that are preliminary or of specialized interest, e.g., quick release reports, working papers, and bibliographies that contain minimal annotation. Does not contain extensive analysis.
- **CONTRACTOR REPORT.** Scientific and technical findings by NASA-sponsored contractors and grantees.

- **CONFERENCE PUBLICATION.** Collected papers from scientific and technical conferences, symposia, seminars, or other meetings sponsored or cosponsored by NASA.
- **SPECIAL PUBLICATION.** Scientific, technical, or historical information from NASA programs, projects, and missions, often concerned with subjects having substantial public interest.
- **TECHNICAL TRANSLATION.** English-language translations of foreign scientific and technical material pertinent to NASA's mission.

Specialized services that complement the STI Program Office's diverse offerings include creating custom thesauri, building customized data bases, organizing and publishing research results . . . even providing videos.

For more information about the NASA STI Program Office, see the following:

- Access the NASA STI Program Home Page at <http://www.sti.nasa.gov>
- E-mail your question via the Internet to help@sti.nasa.gov
- Fax your question to the NASA Access Help Desk at (301) 621-0134
- Telephone the NASA Access Help Desk at (301) 621-0390
- Write to:
NASA Access Help Desk
NASA Center for AeroSpace Information
7121 Standard Drive
Hanover, MD 21076



Numerical Analysis of the Trailblazer Inlet Flowfield for Hypersonic Mach Numbers

C.J. Steffen, Jr. and J.R. DeBonis
Glenn Research Center, Cleveland, Ohio

Prepared for the
38th Aerospace Sciences Meeting and Exhibit
sponsored by the American Institute of Aeronautics and Astronautics
Reno, Nevada, January 10-13, 2000

National Aeronautics and
Space Administration

Glenn Research Center

Available from

NASA Center for Aerospace Information
7121 Standard Drive
Hanover, MD 21076
Price Code: A03

National Technical Information Service
5285 Port Royal Road
Springfield, VA 22100
Price Code: A03

NUMERICAL ANALYSIS OF TRAILBLAZER INLET FLOWFIELD FOR HYPERSONIC MACH NUMBERS

C.J. Steffen, Jr.⁺ and J.R. DeBonis⁺
Turbomachinery and Propulsion Systems Division
National Aeronautics and Space Administration
Glenn Research Center
Cleveland, Ohio 44135

Abstract

A study of the Trailblazer vehicle inlet was conducted using the GASP code for flight Mach numbers ranging from 4-12. Both perfect gas and finite rate chemical analysis were performed with the intention of making detailed comparisons between the two results. Inlet performance was assessed using total pressure recovery and kinetic energy efficiency. These assessments were based upon a one-dimensional stream-thrust-average of the axisymmetric flowfield. Flow visualization was utilized to examine the detailed shock structures internal to this mixed-compression inlet. Kinetic energy efficiency appeared to be the least sensitive to differences between the perfect gas and finite rate chemistry results. Total pressure recovery appeared to be the most sensitive discriminator between the perfect gas and finite rate chemistry results for flight Mach numbers above Mach 6. Adiabatic wall temperature was consistently overpredicted by the perfect gas model for flight Mach numbers above Mach 4. The predicted shock structures were noticeably different for Mach numbers from 6-12. At Mach 4, the perfect gas and finite rate chemistry models collapse to the same result.

Introduction

NASA is presently studying several advanced propulsion systems that promise to provide affordable access to space. The John H. Glenn Research Center is focusing on the development and demonstration of several low-risk approaches to Air-Breathing Launch Vehicle technologies. One concept, known as the Trailblazer spacecraft¹, is based upon Rocket Based Combined Cycle (RBCC) propulsion. A three view schematic is shown in figure 1. Vehicle propulsion is the critical technology for the Trailblazer program. However, design simplicity is the key attribute. Therefore, a nearly axisymmetric

engine design has been created. Structural and analytical simplicity results, as shown in figures 1 and 2.

The mission for Trailblazer is access to space. An accelerating, trans-atmospheric trajectory places large demands upon an air-breathing propulsion system. In particular, the compression system must function effectively across a large operating range. The RBCC concept considered here is defined by four separate modes in a single-stage-to-orbit configuration. First, the engine functions with the rocket ignited in the Independent Ramjet Stream (IRS) cycle² of operation (mode 1). Then the rocket engine is switched off and subsonic combustion is present in the ramjet (mode 2). As the vehicle continues to accelerate, supersonic combustion occurs in the scramjet (mode 3). The rocket is eventually re-ignited (mode 4) for the final ascent into orbit in an all-rocket configuration. Further details on the operation of this propulsion cycle are available in reference 1. The Trailblazer compression system is primarily based upon the translating centerbody inlet design. A small amount of initial compression from the vehicle forebody is developed as well. An analysis of this forebody compression is addressed in the previous work of reference 3.

Analysis of the Trailblazer inlet performance involved three closely related efforts. First, a series of numerical simulations were conducted, based upon the calorically perfect gas assumption³. This effort constituted the initial design and analysis phase. Flight Mach numbers from [0.5-12.0] were examined for a variety of translating spike positions. Next, a second series of numerical simulations were conducted using finite rate chemical kinetics models (FRC), and equilibrium thermodynamic assumptions. This effort concentrated upon the hypersonic flight conditions in order to quantify the

⁺ Senior Member AIAA

aerothermodynamic effects upon the Trailblazer inlet performance predictions. Axisymmetric calculations were executed. The present work is a documentation of this second series of numerical simulations. Finally, an eight-percent scale model of the Trailblazer inlet was fabricated. Testing is currently underway in the NASA Glenn 1'x1' supersonic wind tunnel. Inlet performance data will be gathered for a Mach number range of [2.5-6.0]. Together, these three coordinated efforts will help to quantify the inlet performance, which in turn will be used to further optimize the flight trajectory, cycle analysis and flowpath design.

A series of axisymmetric FRC simulations were executed with the General Aerodynamic Simulation Program (GASP) to assess the compression performance as a function of flight Mach number for a nominal Trailblazer trajectory during hypersonic flight. Mach numbers ranged from [4.0-12.0], while the altitude spanned [62kft-114kft]. Additionally, a series of perfect gas (PG) simulations were executed with the same flow solver at the same flow conditions and meshes to permit direct comparisons between these numerical modeling assumptions. This comparison will be used in future analyses to determine which level of aerothermodynamic modeling is required for more intensive three-dimensional CFD analysis.

Governing Assumptions

For the purposes of this study, axisymmetric analysis was deemed sufficient. The three-dimensional effects of the flowpath endwalls will be addressed in a future study, in conjunction with the aforementioned supersonic wind tunnel tests. The flow at station one is assumed to have traversed the forebody shock, and re-expanded to the freestream static pressure. The total temperature is assumed to remain constant across the forebody shock wave. The freestream and total conditions specified at station one for this study are given in table 1. As shown earlier in reference 3, this is a conservative estimate of overall compression performance, but suffices for the axisymmetric flows simulated herein. The simulations for Mach 6, 8, 10, and 12 were performed with an inlet configured to yield a contraction ratio of 16. The simulations for Mach 4 were conducted at contraction ratio of 8. The computational domain extended from just forward of station #1, downstream to the inlet throat at station #2. The inlet throat is defined by the downstream facing step, visible in figure 2. This discontinuous area distribution was designed to isolate the forward portion of the inlet from the pressure changes of the combustor, and provide a location for axial fuel injection. The calculations of reference 3 have demonstrated that the flowfield upstream of the throat was unaffected by

changes in the combustor region backpressure. Thus the numerical domain for the present study has been truncated at station #2.

The performance data presented below were based upon a one-dimensional stream thrust averaging of the axisymmetric solution. Riggins and McClinton⁴ have presented the details of applying this averaging procedure to FRC calculations. Once the one dimensional flow average has been computed, it can be compared to a reference condition in order to assess the compression system performance. For the present work, we have chosen to present the performance in terms of the total pressure recovery $\left(\frac{P_{02}}{P_{01}}\right)$ and kinetic energy efficiency (η_{ke}) . For the PG simulations, one can compute the reference stagnation and expansion states directly from the stream thrust averaged state. However, for the FRC simulations, we have applied the Chemical Equilibrium with Applications (CEA) code of Gordon and McBride⁵ to compute first the local chemical equilibrium condition, then the isentropic equilibrium stagnation condition, and finally the isentropic equilibrium expansion to the freestream pressure condition.

Numerical Modeling

The flow solver GASP v3.2⁶ from Aerosoft, Inc. was used to conduct the analysis. The solver was configured to the following specifications:

- Third-order-accurate upwind biased scheme
- Van Albada limiting strategy
- Two-factor ADI algorithm
- Roe's approximate Reimann solver
- Low Re, $k-\omega$ turbulence model
- Kang and Dunn model⁷ for the chemical kinetics
- Thermodynamic equilibrium assumed for translational, rotational, and vibrational energy modes

The mesh was developed with Gridgen⁸ software from Pointwise, Inc. The mesh consisted of 300 cells axially by 45 cells radially. The numerical domain covered a region forward of the inlet spike tip down through the inlet throat section. The surfaces of the inlet were modeled by a no-slip adiabatic wall boundary condition. The freestream was fixed as supersonic inflow; the outflow at the throat was fixed as an extrapolation condition. The simulations of Mach 4 and Mach 6 indicated that the inlet spilled a portion of the flow compressed by the centerbody. The upper boundary, forward of the cowl, must account for the exiting of a

subsonic radial component of flow. This boundary was modeled as a Riemann outflow condition. For the Mach 8 through Mach 12 conditions, no spilling occurred and this boundary was fixed at the freestream condition.

An additional calculation was performed for the Mach 10 FRC simulation on a fine mesh consisting of 600 cells axially by 90 cells radially to assess the mesh dependence of the results. The comparative analysis revealed that the standard mesh and fine mesh results were essentially the same. Table 2 shows the stream thrust averaged data at station #2. Notice that the total pressure recovery data agree to within 0.2%. Thus we felt confident that the standard mesh was of sufficient size to yield a grid independent solution for the stream thrust averaged data.

Results

The experimental matrix consisted of two aerothermodynamic model calculations at 5 different flight conditions. The flight condition data shown in table 1 are representative of the vehicle trajectories studied to date. Compression system performance has been presented both in terms of total pressure recovery and kinetic energy efficiency. Both of these measures relied upon an integral result of the inlet flowfield at the throat. However, adiabatic wall temperature also presented another interesting comparison between the two aerothermodynamic model results. All three comparisons are presented below in table 1.

Graphical comparisons between the FRC and PG results for total pressure recovery and kinetic energy efficiency are shown in figure 3. Notice that the general trend of decreasing inlet performance with increasing Mach number was captured by both performance parameters for the PG and FRC calculations. Another interesting way to compare these results involved taking the ratio of the PG and FRC performance parameters. This data is displayed in figure 4 for both performance parameters and the adiabatic wall temperature at the inlet throat. Complete agreement between the PG and FRC data would result in a ratio of 100%. This was observed for all three curves of figure 4 at a Mach number of 4. Note that total pressure recovery results agreed quite well for a flight Mach number of 6 or lower. However, the results diverge quickly above Mach 6, and by Mach 12, the PG result has over-predicted the recovery by 42%. The kinetic energy efficiency was actually insensitive to the differences between the FRC and PG results. Even at Mach 12, the two results agreed to within 1%. This apparent paradox underscores the difference in sensitivity of these two compression performance parameters for hypersonic flow. Heiser and Pratt discuss this difference in sensitivity during a lengthy discussion

of compression system performance*. Other factors that complicate this comparison between PG and FRC total pressure recovery involve the difficulty of stagnating hypersonic flows. The differences between the reference stagnation states using the PG and chemical equilibrium assumptions can be significant. Finally, consider that an extra entropy increase is unavoidable during the step from a stream thrust averaged chemical non-equilibrium state to chemical equilibrium at the same pressure and temperature. Notwithstanding these observations, the data of figure 4 indicate two specific conclusions: 1) the FRC and PG results collapse to the same values at a Mach number of 4, 2) the difference in compression performance between the FRC and PG results was exaggerated by the total pressure recovery and minimized by the kinetic energy efficiency.

The adiabatic wall temperature at the throat was steadily over-predicted by the PG mode above Mach 4, with a 25% error at Mach 12. A plot of the adiabatic wall temperature as a function of axial location along the inlet centerbody is shown in figure 5. It is clear that the predicted heat load of the PG simulation will be significantly over-predicted above Mach 4.

It is well known that for hypersonic flight analysis, the calorically perfect gas assumption will begin to break down with temperatures that exceed the onset of vibrational excitation. This occurs at approximately 1400R*. At temperatures of approximately 4500R, oxygen molecules begin to dissociate, and by 7200R the nitrogen will begin to dissociate. For our vehicle trajectory, one would expect to encounter erroneous stagnation temperatures at speeds above Mach 4. However, the stream thrust averaging technique mixed the hot boundary layer and relatively cool core flows together so that at Mach 4, the adiabatic wall temperature was approximately 500R hotter than the integrated temperature of 1030R across the inlet throat. By Mach 6, the adiabatic wall temperature and the stream thrust averaged temperatures were 2723R and 1850R, respectively. Thus, performance measures that rely upon the integrated stream thrust average will not be expected to reveal a significant difference between PG and FRC performance until the average temperature rises into the range of vibrational excitation. This appears to occur at about Mach 6 for our trajectory.

The evidence of a boundary layer separation along the centerbody is visible in the data of figure 5 for Mach numbers 8, 10, and 12. The Mach number contours of figure 6 depict this separation more clearly. This vehicle

* These temperature ranges are based upon an equilibrium condition at a pressure of 1 atmosphere.

was designed to operate for an ascent trajectory; thus the compression system was expected to operate over the entire air-breathing portion of the trajectory. However, the inlet was designed for a shock on lip at Mach 6. Figure 6 d) shows that inlet was actually spilling slightly, but the shock emanating from the cowl was cancelled by the local turning at the centerbody wall. From the contours of figure 6, you can see that the Mach 8,10, and 12 flight conditions are oversped and result in a strong reflected shock wave that encounters the centerbody boundary layer downstream of an expansion region.

The internal portion of the compression system is dominated by the presence of strong, reflected shock waves, as might be expected. These shocks were revealed best by imaging the natural logarithm of the magnitude of the density gradient. This technique produces an image similar to the experimental Schlieren technique. Figure 7 reveals the largest shock and shear layer structures that were present in the internal flowfields for the FRC simulations. Notice again that when the shock-boundary layer interaction occurred downstream of the centerbody expansion region, a large separation region resulted. Figure 8 revealed similar details about the perfect gas simulations, and permitted an interesting comparison of the detailed shock structures between the FRC and PG results.

Note that the shock trains of figure 7 were more elongated than their counterparts of figure 8. This qualitative difference was discernible for the results of Mach 6-12. This elongated shock train indicated that a higher Mach number flow through the internal compression region of the inlet was present for the FRC result, when compared to the PG result. Indeed, the FRC throat Mach number of 2.52 was substantially greater than the PG throat Mach number of 2.00, for the Mach 12 flight condition. At Mach 4, the results appeared essentially identical. This result indicates that the accurate prediction of local shock phenomena, including boundary layer separation and consequent heat transfer, will necessitate FRC calculations for flight Mach numbers of 6 and above.

Conclusions

Future CFD calculations are necessary during the technology maturation phase of the Trailblazer vehicle project. The present work can be used to discriminate between two approaches to executing the CFD analysis: the relatively inexpensive perfect gas simulation of compressing air, and the more expensive and accurate finite rate chemistry approach which incorporates the equilibrium vibrational energy model.

1. Kinetic energy efficiency was not sensitive to differences between the PG and FRC results for flight Mach numbers in the range of 4-12.
2. Total pressure recovery was the most sensitive discriminator between the PG and FRC results for flight Mach numbers above Mach 6. For flight at or below Mach 6, the total pressure recovery results were nearly identical.
3. The PG model consistently overpredicted adiabatic wall temperature for flight Mach numbers above 4. This was expected with the breakdown of the calorically perfect gas assumption. At Mach 4, the temperature results are nearly identical; at Mach 12, the temperature results differ by nearly 2000R.
4. Discernible differences were apparent in a comparison of the shock structures of the PG and FRC results for flight Mach numbers of 6 and above. Accurate prediction of local shock phenomena, including boundary layer separation and consequent heat transfer will necessitate FRC simulations in this Mach number range.

For the Trailblazer vehicle and trajectory presented, Mach 4 corresponds to the flight condition at which the boundary layer temperatures begin to reach levels that exceed the range of validity for the calorically perfect gas assumption. We expect this Mach number threshold to apply to a wide variety of hypersonic inlet configurations with similar trajectories.

References

- ¹Trefny, C. J. "An Airbreathing Launch Vehicle Concept for Single Stage to Orbit," AIAA 99-2730, 35th AIAA/ASME/SAE/ASEE Joint Propulsion Conference and Exhibit, June 20-23, 1999
- ²Yungster, S., and Trefny, C. J., "Analysis of a New Rocket-Based Combined-Cycle Engine Concept at Low Speed," AIAA 99-2393, , 35th AIAA/ASME/SAE/ASEE Joint Propulsion Conference and Exhibit, June 20-24, 1999.
- ³Debonis, J. R., Trefny, C. J. and Steffen, C. J. Jr., "Inlet Development for a Rocket Based Combined Cycle, Single Stage to Orbit Vehicle Using Computational Fluid Dynamics," AIAA 99-2239, 35th AIAA/ASME/SAE/ASEE Joint Propulsion Conference and Exhibit, June 20-24, 1999
- ⁴Riggins, D. W., and McClinton, C. R., "Analysis of Losses in Supersonic Mixing and Reacting Flows," AIAA 91-2266, 27th AIAA/ASME/SAE/ASEE Joint Propulsion Conference and Exhibit, June 24-26, 1991
- ⁵Gordon, S. and McBride, B. J., "Computer Program for Calculation of Complex Chemical Equilibrium Compositions and Applications; Part I. Analysis," NASA Reference Publication 1311, October 1994, Cleveland, OH

⁶GASP Version 3, User's Manual, ISBN 0-9652780-0-X, Aerosoft, Inc., 1996, Blacksburg, VA

⁷Kang, S. -W., Dunn, M. G., and Jones, W. L., "Theoretical and Measured Electron Density Distributions for the RAM Vehicle and high Altitudes." AIAA 72-689, AIAA 5th fluid and Plasma Dynamics Conference, June, 1972.

⁸ Gridgen Version 13, User Manual, Pointwise, Inc., 1998, Bedford, Texas.

⁹Heiser, W. H. and Pratt, D. T., Hypersonic Airbreathing Propulsion, AIAA Education series, ISBN 1-56347-035-7, 1994.

Table 1. Simulated flight conditions and performance results for the calorically perfect gas model (PG) and the finite rate chemistry model (FRC) at five different points on the trajectory.

CFD Model	Flight Condition		Station #1 Mach #	P ₀ Recovery		Kinetic Energy Efficiency		Throat Temp. At wall (R)	
	Mach #	Altitude		$\frac{P_{02}}{P_{01}}$	PG/FRC	η_{ke}	PG/FRC	T _{wall}	PG/FRC
PG	4	62000	3.994	66.5%	102%	95.9%	101%	1551	104%
FRC				65.4%		95.3%		1495	
PG	6	84110	5.933	40.0%	103%	94.9%	100%	2956	109%
FRC				38.9%		94.8%		2723	
PG	8	96440	7.750	16.0%	111%	92.7%	100%	4944	114%
FRC				14.3%		92.7%		4318	
PG	10	107100	9.397	6.62%	126%	91.7%	101%	7314	119%
FRC				5.22%		90.8%		6158	
PG	12	114500	10.857	3.31%	142%	91.3%	101%	9454	125%
FRC				2.32%		90.6%		7538	

Table 2. Results of the mesh dependence study of the Mach 10 FRC simulation.

Mesh Dependence Analysis			
Data at Station #2	Standard mesh result	Fine mesh result	Δ%
Stream Thrust Averaged Pressure	2953.4 psf	2900.7 psf	1.8%
Stream Thrust Averaged Temperature	3535.4 R	3518.1 R	0.5%
Stream Thrust Averaged Velocity	6670.2 fps	6698.5 fps	0.3%
Total Pressure Recovery	5.22%	5.21%	0.2%

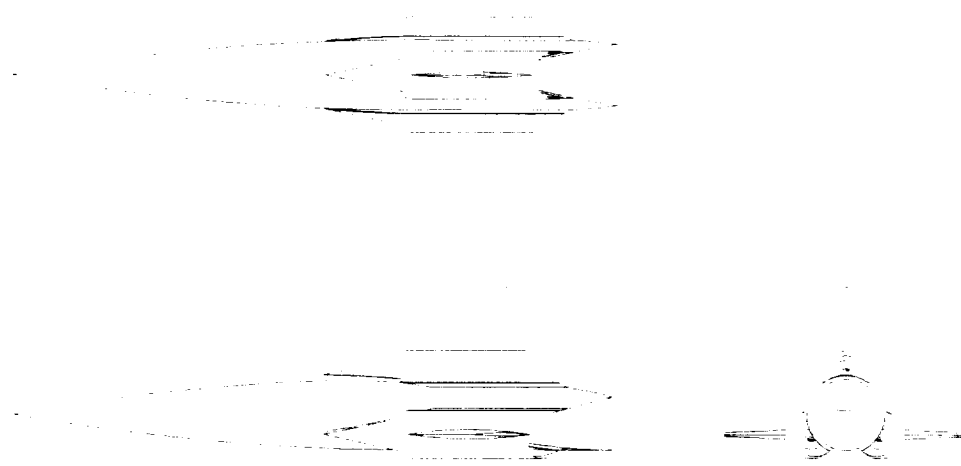


Figure 1. Three view schematic of the Trailblazer vehicle.

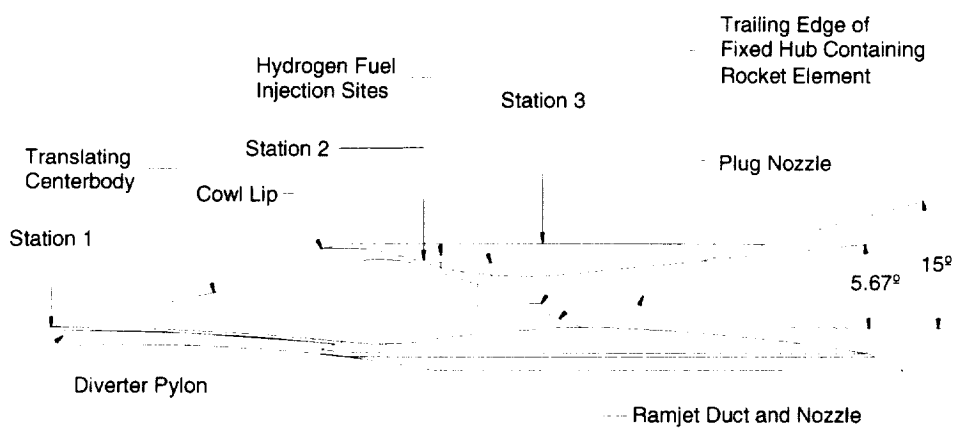


Figure 2. Cut-away view of the Trailblazer engine.

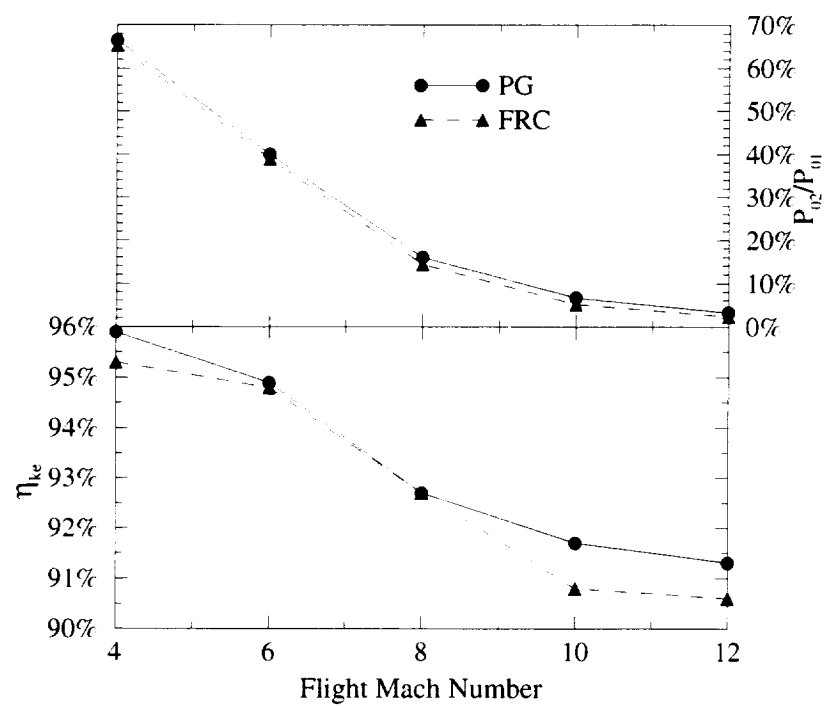


Figure 3. Perfect Gas (PG) to Finite Rate Chemistry (FRC) performance comparisons for Mach 4-12 flight.

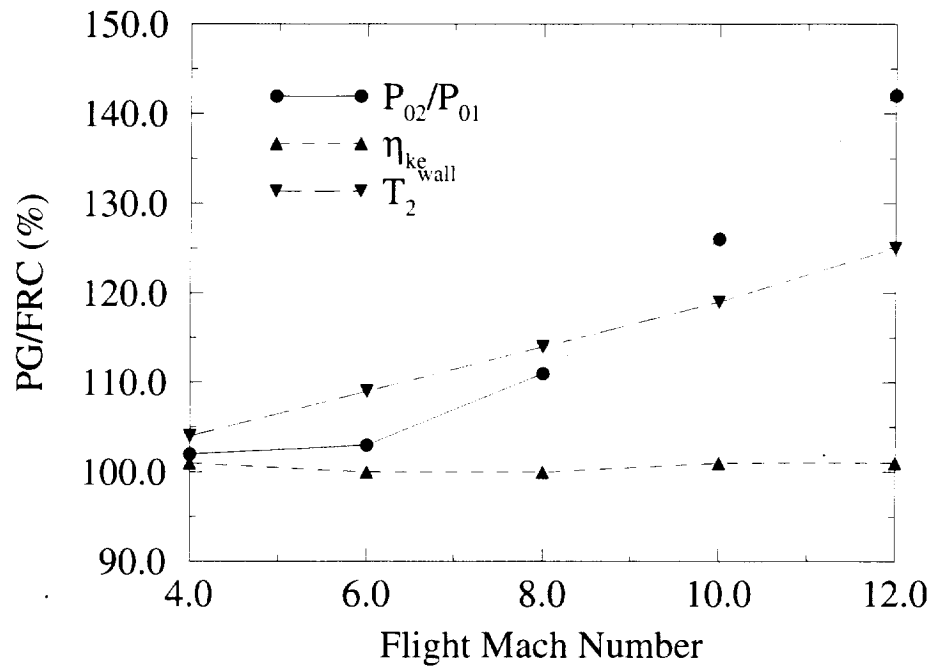


Figure 4. Ratio of Perfect Gas (PG) to Finite Rate Chemistry (FRC) compression performance and wall temperature for Mach 4-12 flight.

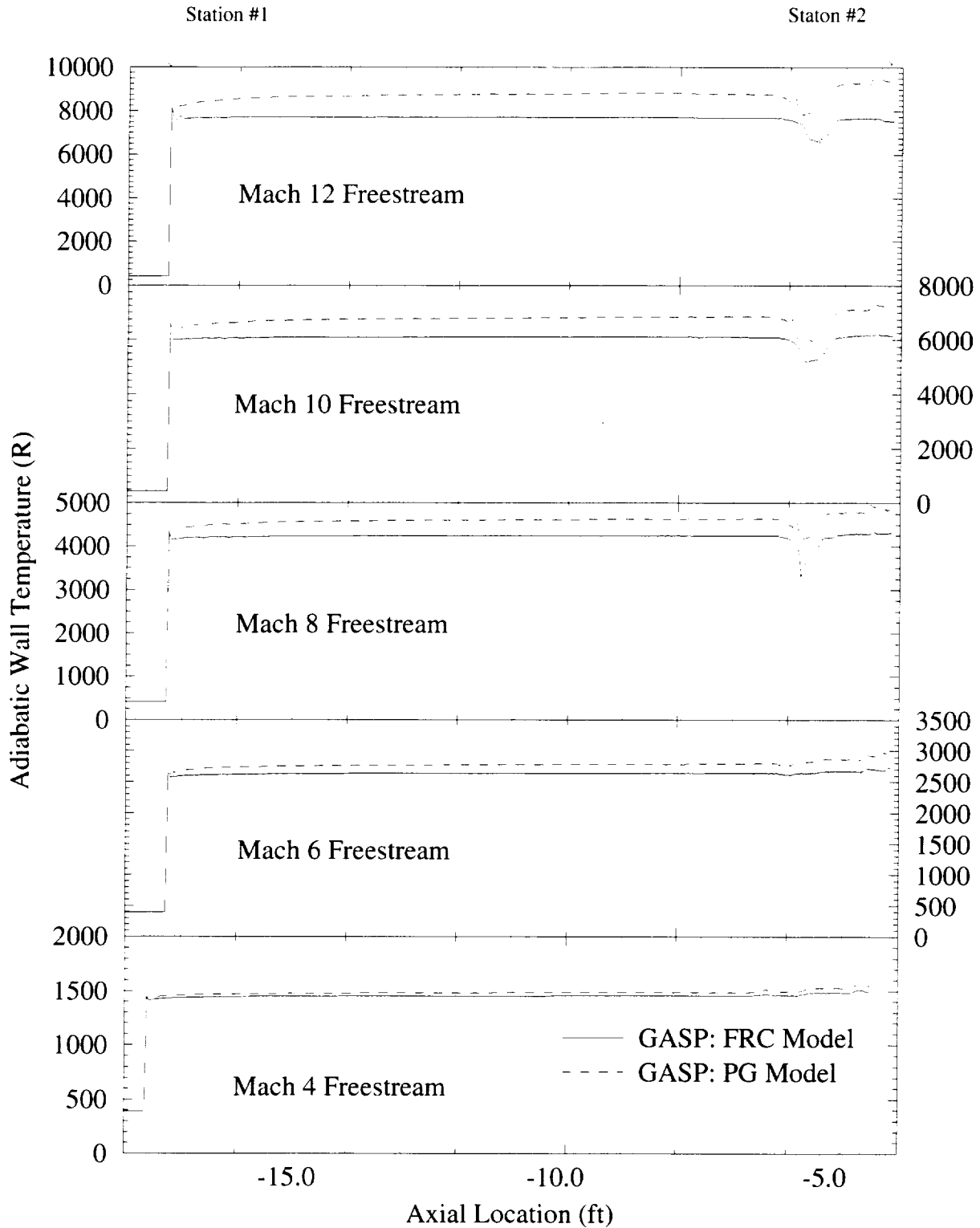


Figure 5. Adiabatic wall temperature profile comparisons along the inlet centerbody for Mach 4-12 flight.

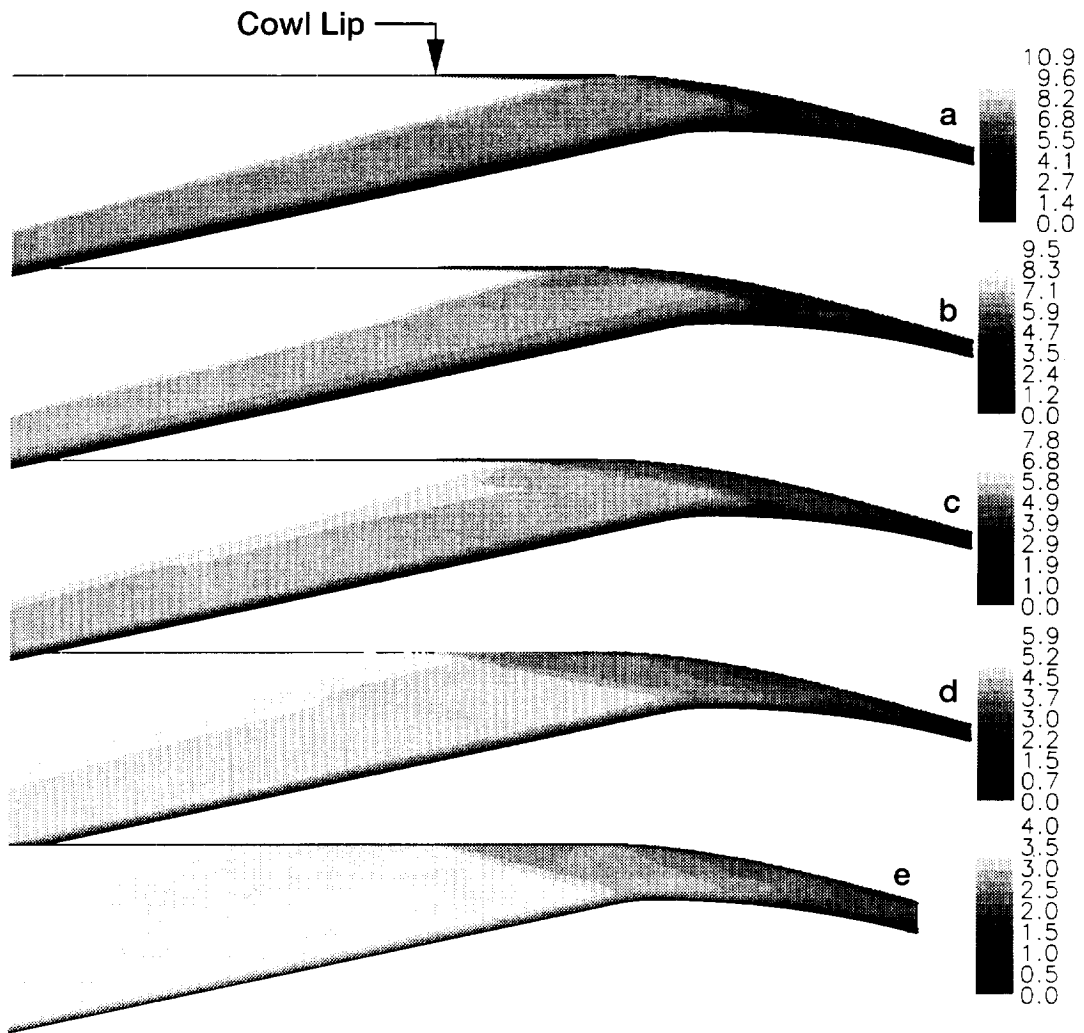


Figure 6. Mach number contours: (a) Mach 12, (b) Mach 10, (c) Mach 8, (d) Mach 6, and (e) Mach 4. Note the shock induced flow separations along the centerbody for Mach 8-12.

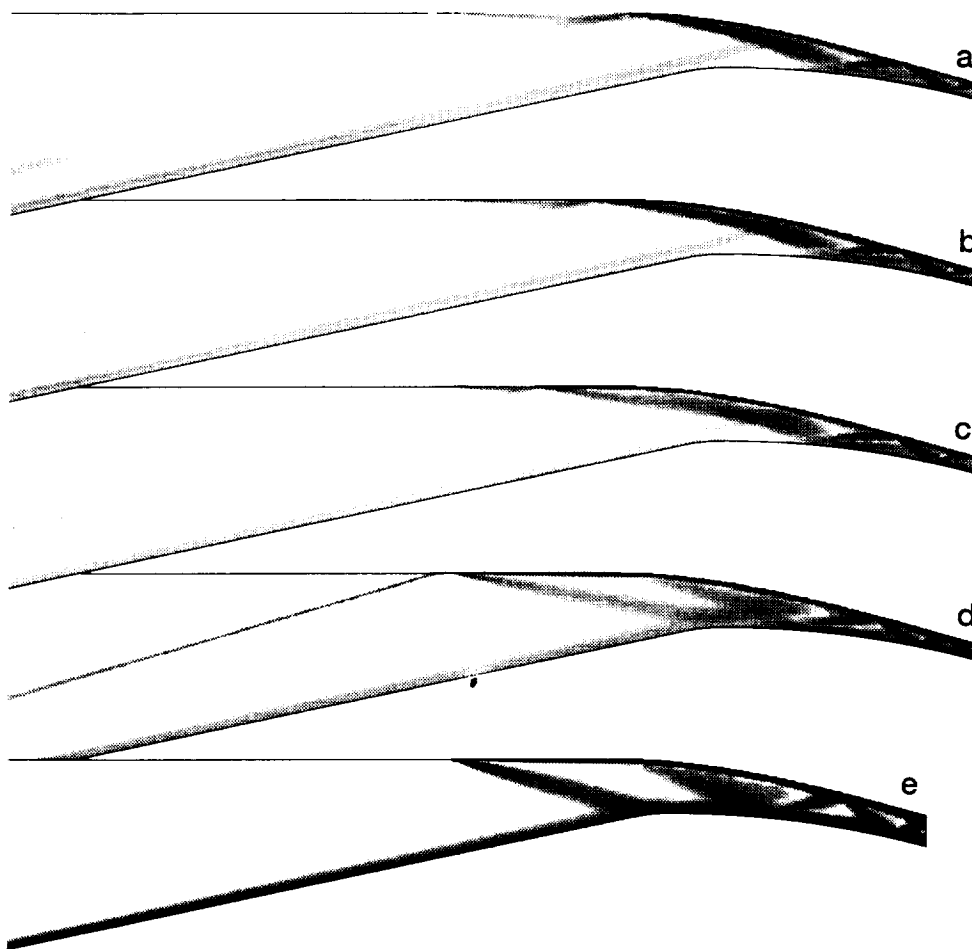


Figure 7. Numerical Schlieren images of the FRC simulations: (a) Mach 12, (b) Mach 10, (c) Mach 8, (d) Mach 6, and (e) Mach 4. Note the complex reflecting shock structures internal to this mixed compression inlet.

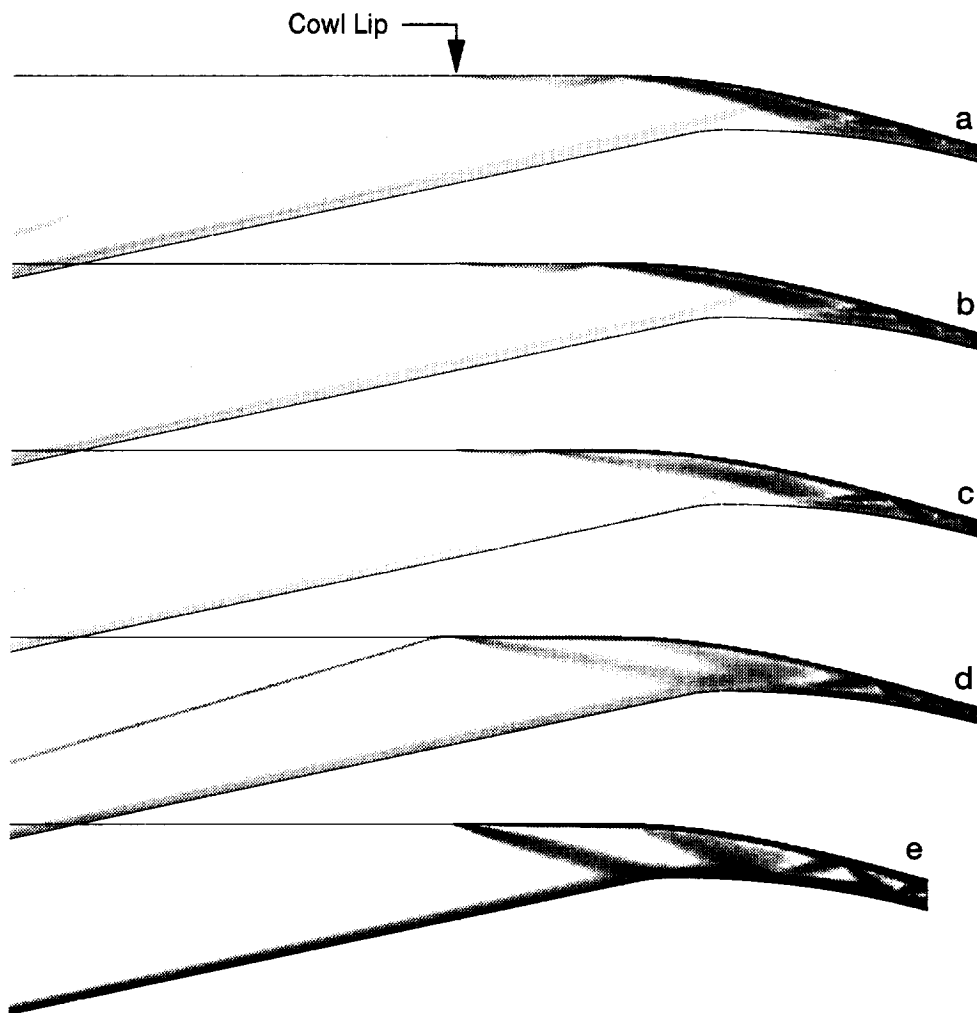


Figure 8. Numerical Schlieren images of the PG simulations: (a) Mach 12, (b) Mach 10, (c) Mach 8, (d) Mach 6, and (e) Mach 4. Note the differences between the previous images of figure 6 for Mach Numbers 6-10. The multiple reflected shock angles of this image appear to be steeper by comparison.

REPORT DOCUMENTATION PAGE

Form Approved
OMB No. 0704-0188

Public reporting burden for this collection of information is estimated to average 1 hour per response, including the time for reviewing instructions, searching existing data sources, gathering and maintaining the data needed, and completing and reviewing the collection of information. Send comments regarding this burden estimate or any other aspect of this collection of information, including suggestions for reducing this burden, to Washington Headquarters Services, Directorate for Information Operations and Reports, 1215 Jefferson Davis Highway, Suite 1204, Arlington, VA 22202-4302, and to the Office of Management and Budget, Paperwork Reduction Project (0704-0188), Washington, DC 20503.

1. AGENCY USE ONLY (<i>Leave blank</i>)	2. REPORT DATE December 1999	3. REPORT TYPE AND DATES COVERED Technical Memorandum	
4. TITLE AND SUBTITLE Numerical Analysis of the Trailblazer Inlet Flowfield for Hypersonic Mach Numbers		5. FUNDING NUMBERS WU-523-31-13-00	
6. AUTHOR(S) C.J. Steffen, Jr. and J.R. DeBonis			
7. PERFORMING ORGANIZATION NAME(S) AND ADDRESS(ES) National Aeronautics and Space Administration John H. Glenn Research Center at Lewis Field Cleveland, Ohio 44135-3191		8. PERFORMING ORGANIZATION REPORT NUMBER E-12010	
9. SPONSORING/MONITORING AGENCY NAME(S) AND ADDRESS(ES) National Aeronautics and Space Administration Washington, DC 20546-0001		10. SPONSORING/MONITORING AGENCY REPORT NUMBER NASA TM-1999-209654 AIAA-2000-0889	
11. SUPPLEMENTARY NOTES Prepared for the 38th Aerospace Sciences Meeting & Exhibit sponsored by the American Institute of Aeronautics and Astronautics, Reno, Nevada, January 10-13, 1999. Responsible person, C.J. Steffen, Jr., organization code 5880, (216) 433-8508.			
12a. DISTRIBUTION/AVAILABILITY STATEMENT Unclassified - Unlimited Subject Categories: 02 and 64 This publication is available from the NASA Center for AeroSpace Information, (301) 621-0390.		12b. DISTRIBUTION CODE Distribution: Nonstandard	
13. ABSTRACT (<i>Maximum 200 words</i>) A study of the Trailblazer vehicle inlet was conducted using the GASP code for flight Mach numbers ranging from 4-12. Both perfect gas and finite rate chemical analysis were performed with the intention of making detailed comparisons between the two results. Inlet performance was assessed using total pressure recovery and kinetic energy efficiency. These assessments were based upon a one-dimensional stream-thrust-average of the axisymmetric flowfield. Flow visualization was utilized to examine the detailed shock structures internal to this mixed-compression inlet. Kinetic energy efficiency appeared to be the least sensitive to differences between the perfect gas and finite rate chemistry results. Total pressure recovery appeared to be the most sensitive discriminator between the perfect gas and finite rate chemistry results for flight Mach numbers above Mach 6. Adiabatic wall temperature was consistently overpredicted by the perfect gas model for flight Mach numbers above Mach 4. The predicted shock structures were noticeably different for Mach numbers from 6-12. At Mach 4, the perfect gas and finite rate chemistry models collapse to the same result.			
14. SUBJECT TERMS Aerodynamics; Numerical analysis		15. NUMBER OF PAGES 17	
		16. PRICE CODE A03	
17. SECURITY CLASSIFICATION OF REPORT Unclassified	18. SECURITY CLASSIFICATION OF THIS PAGE Unclassified	19. SECURITY CLASSIFICATION OF ABSTRACT Unclassified	20. LIMITATION OF ABSTRACT